

Single massive stars at the critical rotational velocity: possible links with Be and B[e] stars

Georges Meynet and André Maeder

Geneva Observatory

Abstract. Using single star models including the effects of shellular rotation with and without magnetic fields, we show that massive stars at solar metallicity with initial masses lower than about $20-25 M_{\odot}$ and with an initial rotation above $\sim 350 \text{ km s}^{-1}$ likely reach the critical velocity during their Main-Sequence phase. This results from the efficient outwards transport of angular momentum by the meridional circulation. This could be a scenario for explaining the Be stars. After the Main-Sequence phase, single star in this mass range can again reach the critical limit when they are on a blue loop after a red supergiant phase (Heger & Langer 1998). This might be a scenario for the formation of B[e] stars, however as discussed by Langer & Heger (1998), this scenario would predict a short B[e] phase (only some 10^4 years) with correspondingly small amounts of mass lost.

1. Link between Be, B[e] supergiants stars and rotation

A common feature of Be and B[e] supergiants is the non-sphericity of their circumstellar envelopes (see e.g. the review by Zickgraf 2000). More precisely, in both cases, disks are supposed to be present, likely disk of outflowing material. How do these disk form ? How long are their lifetimes ? Are they intermittent ? Are they Keplerian ? Many of these questions have been discussed in this conference and are still subject of lively debate. A point however which seems well accepted is the fact that the origin of an axisymmetric wind structure such as a disk might be connected to the fast rotation of the star (Pelupessy et al. 2000). If correct, this connection between fast rotation and the Be and B[e] phenomena leads to the question, when such fast rotation can be encountered in the course of the evolution of massive single stars ? In this paper, we give some elements of answer to that question based on models accounting for the effects of shellular rotation (Zahn 1992).

2. The critical velocity

The critical angular velocity corresponds to the angular velocity at the equator of the star such that the centrifugal force exactly balances the gravity. The critical angular velocity $\Omega_{\text{crit},1}$ in the frame of the Roche model for computing the gravity due to the deformed star, is given by

$$\Omega_{\text{crit},1} = \left(\frac{2}{3}\right)^{\frac{3}{2}} \left(\frac{GM}{R_{\text{pc}}^3}\right)^{\frac{1}{2}}, \quad (1)$$

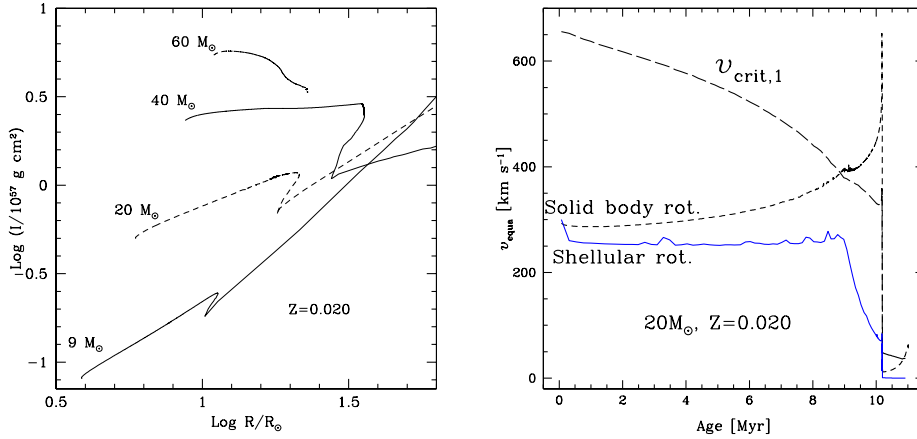


Figure 1. *Left* : Evolution of the total momentum of inertia of different stellar models at solar metallicity. The hook along the tracks corresponds to the end of the Main Sequence phase. Only the beginning of the track is shown for the $60 M_\odot$ stellar model. *Right* : The continuous line shows Evolution of the surface velocity of a $20 M_\odot$ at solar metallicity with $v_{\text{ini}} = 300 \text{ km s}^{-1}$ according to the models computed by Meynet & Maeder (2003). The long-dashed line corresponds to the critical velocity given by Eq. 1. The short-dashed line shows the surface velocity the star would have, if solid body rotation is assumed.

where R_{pc} is the polar radius when the surface rotates with the critical velocity.

Looking at Eq. (1), one can be surprised that the stellar luminosity does not appear. Indeed, we could expect that, in addition to the centrifugal acceleration, the radiative acceleration would help in balancing the gravity. When the stellar luminosity is sufficiently far from the Eddington limit (see below for a more precise statement), it has been shown by Glatzel (1998) and Maeder & Meynet (2000) that radiative acceleration does not play any role. Physically, this comes from the fact that when the star reaches the critical limit at the equator, the effective gravity (gravity decreased by the effect of the centrifugal acceleration) becomes zero there and the radiative flux, responsible for the radiative acceleration, tends also toward zero due to the von Zeipel theorem (von Zeipel 1924; Maeder 1999).

In contrast, when the stellar luminosity approaches the Eddington limit, the radiative acceleration becomes a dominant effect. Why such a difference between the case far from the Eddington limit and the case near the Eddington limit ? One could indeed argue that even near the Eddington limit, when the critical limit is approached, the radiative flux becomes zero at the equator. This is correct, but another mechanism comes into play here: the fact that the Eddington limit is modified when the star is rotating. Let us first recall that the classical Eddington luminosity is given by the expression

$$L_{\text{Edd}} = 4\pi cGM/\kappa, \quad (2)$$

where κ is the total opacity, L the luminosity, M the mass of the star and the other symbols have their usual meanings. Now, when the star is rotating, two

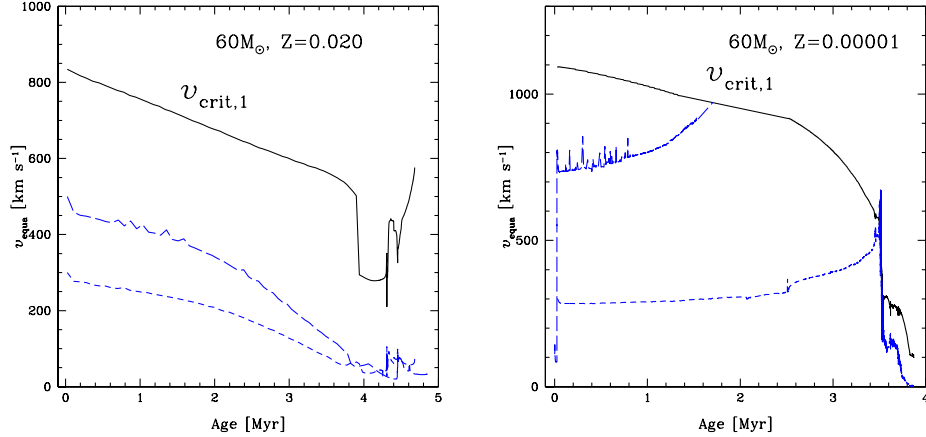


Figure 2. *Left* : Evolution of the surface equatorial velocities at the surface of $60 M_{\odot}$ models at solar metallicity with $v_{\text{ini}} = 300$ (short-dashed line) and 500 km s^{-1} (long-dashed line). The continuous line shows the evolution of the equatorial critical velocity given by Eq. (1). *Right* : Same as the left part of the figure, for $60 M_{\odot}$ at $Z = 10^{-5}$ with $v_{\text{ini}} = 300$ (short-dashed line) and 800 km s^{-1} (long-dashed line).

important differences appear: first the Eddington limit varies as a function of the colatitude θ , second, it is decreased when the rotational velocity increases. The Eddington limit modified by rotation is given by (Glatzel 1998; Maeder & Meynet 2000)

$$L_{\text{Edd}}(\Omega) = 4\pi cGM \left(1 - \frac{\Omega^2}{2\pi G\bar{\rho}}\right) / \kappa(\theta), \quad (3)$$

where $\bar{\rho} = M/V(\omega)$ is the average density of the star, $V(\omega)$ being the stellar volume when the star is rotating and ω is the ratio of the angular velocity to the critical angular velocity given in Eq. (1).

Thus, when the star is near the Eddington limit, rotation may sufficiently decrease L_{Edd} to make it equal to the actual luminosity of the star. In that case, we say the star has reached the $\Omega\Gamma$ -limit and strong mass loss ensues.

Now at which velocity does this occur ? To obtain it, one has to find the value of Ω such that $L = L_{\text{Edd}}(\Omega)$, where $L_{\text{Edd}}(\Omega)$ is given by Eq. (3). This is equivalent to find Ω such that

$$\Gamma_{\text{max}} \equiv \frac{\kappa_{\text{max}} L}{4\pi cGM} = 1 - \frac{\Omega^2}{2\pi G\bar{\rho}}, \quad (4)$$

where we have added the subscript “max” to indicate that the critical limit will be reached first at the position on the surface where the opacity is maximum. If the value of Ω satisfying this equality is higher than $\Omega_{\text{crit},1}$ (from now on called the classical limit), then only the classical limit is relevant since it will be reached first. To see if Eq. (4) can be fulfilled with $\Omega < \Omega_{\text{crit},1}$, let us use the definition of $\bar{\rho}$ and of ω to write

$$\frac{\Omega^2}{2\pi G\bar{\rho}} = \frac{16}{81} \omega^2 V'(\omega), \quad (5)$$

with $V'(\omega) = \frac{V(\omega)}{\frac{4}{3}\pi R_{\text{pc}}^3}$. From the Roche model, it can be shown that the quantity $\frac{16}{81}\omega^2 V'(\omega)$ increases from 0 to 0.361 when ω varies from 0 to 1 (see Maeder & Meynet 2000). It means that if Γ_{max} is strictly inferior to $1 - 0.361 = 0.639$, Eq. (4) cannot be fulfilled. If $\Gamma_{\text{max}} = 0.639$, Eq. (4) can be fulfilled with $\Omega = \Omega_{\text{crit},1}$ and if Γ_{max} is superior to 0.639, then values of $\Omega < \Omega_{\text{crit},1}$ can satisfy Eq. (4). A new expression for the critical velocity, valid when the star is sufficiently near the Eddington limit, can be derived. It is given by

$$\Omega_{\text{crit},2} = \left(\frac{9}{4}\right) \Omega_{\text{crit},1} \sqrt{\frac{1 - \Gamma_{\text{max}}}{V'(\omega)}} \quad (6)$$

where $R_e(\omega)$ is the equatorial radius for a given value of the rotation parameter ω . These expressions for the critical velocities are different from the expression

$$\Omega_{\text{crit}} = \Omega_{\text{crit},1}(1 - \Gamma) \quad (7)$$

used by some authors. Expression (7) is correct only if the surface is uniformly bright, which is not the case when the star is rotating fast.

3. Evolution of the surface velocity: two simple extreme cases

The evolution of the rotational velocity at the surface of stars depends mainly on three physical processes:

- The efficiency of the angular momentum transport mechanisms in the interior,
- The movement of expansion/contraction of the surface,
- The mass loss.

An extreme case of internal angular momentum transport is the one which imposes solid body rotation at each time in the course of the evolution of the star. A strong coupling is then realised between the contracting core and the expanding envelope. In that case, the angular velocity Ω is given by the ratio of the total angular momentum J and the total momentum of inertia of the star I . Fig. 1 shows the variation of I as a function of the growing stellar radius for a few stellar models at solar metallicity. In the case of the $9 M_\odot$ model, I varies as R^α with $\alpha \sim 1$. In the case of the $60 M_\odot$ model, α becomes negative. This results from the strong mass loss experienced by this star.

For the $9 M_\odot$, since mass loss by stellar winds remains very modest during the Main Sequence phase, the total angular momentum is conserved during this phase. As a consequence, Ω varies as the inverse of I and since $I \propto R$, $\Omega \propto 1/R$.

From the previous section, we saw that when the star is sufficiently far from the Eddington limit, which is the case for the $9 M_\odot$ stellar model, then $\Omega_{\text{crit},1} \propto R^{-3/2}$. Thus the critical angular velocity decreases more rapidly than the surface angular velocity when the star expands. Clearly this favors the reaching of the critical limit (see also Sackmann and Anand 1970; Langer 1998).

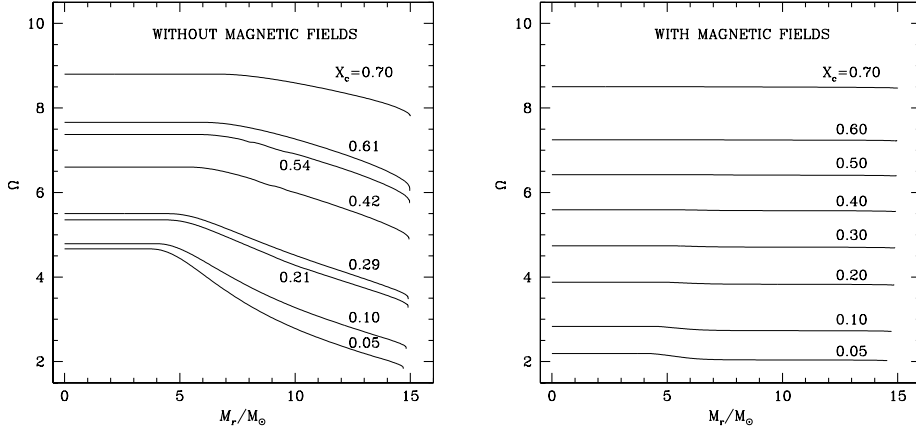


Figure 3. *Left* : Internal distribution of the angular velocity $\Omega(r)$ as a function of the Lagrangian mass in solar units in a $15 M_{\odot}$ model, without magnetic fields, at various stages of the model evolution indicated by the central H-content X_c during the MS-phase. The initial velocity $v_{\text{ini}} = 300 \text{ km s}^{-1}$. *Right* : Same as the left figure but with magnetic fields. One notices the almost constant values of the angular velocity in the models.

To illustrate this last point, let us consider the rotating track for the $20 M_{\odot}$ model (solar metallicity and initial rotational velocity of 300 km s^{-1}) computed by Meynet & Maeder (2003) for obtaining values of the momentum of inertia during the evolution. From these values of I and also using the values for the actual total angular momentum, we deduce the surface velocity that the star would have in case of solid body rotation. We obtain the short dashed line in Fig. 1. Although the model is not self consistently computed (the evolutionary tracks were not computed imposing solid body rotation), it illustrates the fact that indeed when solid body rotation is achieved, the star may reach very easily the critical limit (here represented by the long-dashed line).

Another extreme case is the case of no transport of angular momentum. Each stellar layer keeps its own angular momentum. The variation of Ω is then simply governed by the local conservation of the angular momentum and, at the surface, $\Omega \propto 1/R^2$. When the radius increases, the surface angular velocity decreases more rapidly than the classical critical angular velocity, thus the star evolves away from the critical limit.

Reality is likely in between the cases of solid body rotation and of local conservation of the angular momentum. Let us now see what are the predictions of more physical models.

4. Evolution of the surface velocity in models with shellular rotation

In the interior of stars, at least three mechanisms can transport angular momentum along a radial direction:

- Convection: here we suppose that convective zones have solid body rotation

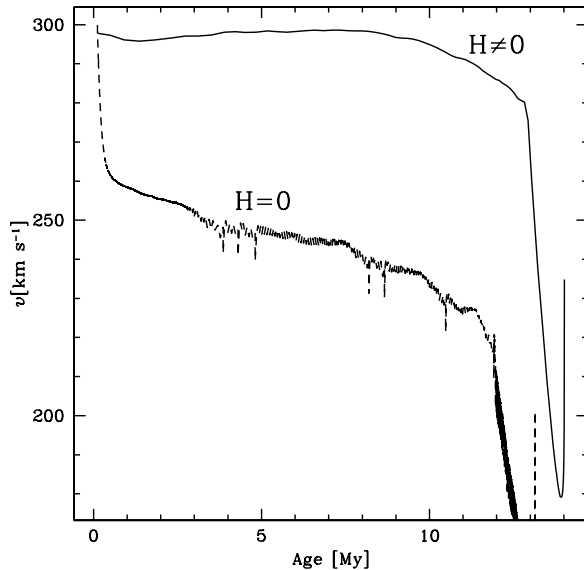


Figure 4. Evolution of the rotation velocities at the surface of $15 M_{\odot}$ models during the MS phase with and without magnetic fields. The initial velocity $v_{\text{ini}} = 300 \text{ km s}^{-1}$ in both cases. We see the much higher surface rotation when magnetic field is included.

- Meridional circulation: this is the main mechanism for the transport of the angular momentum in radiative zones.
- Shear turbulence: only the secular shear turbulence, occurring on thermal timescales, appears to be important. Dynamical shear, occurring on dynamical timescales, appears in the advanced stages of the evolution of massive stars and only affects very locally the profile of Ω (Hirschi et al. 2003). The efficiency of the vertical secular shear turbulence for transporting the angular momentum is in general much smaller than that of the meridional currents.

Let us emphasize that the evolution of the angular velocity inside the star depends on the gradients of the chemical species and of the angular velocity, these gradients being themselves deduced from the variation of Ω as a function of the radius. Thus the problem has to be solved self-consistently, which is done in the computations presented here. More precisely, in the models discussed in this section, the effects of the centrifugal acceleration in the stellar structure equations are accounted for as explained in Kippenhahn & Thomas (1970) (see also Meynet and Maeder 1997). The equations describing the transport of the chemical species and angular momentum resulting from meridional circulation and shear turbulence are given in Zahn (1992) and Maeder & Zahn (1998) (see details on the derivation of the angular momentum transport equation in Meynet & Maeder 2005b). The expressions for the diffusion coefficients are taken from Talon & Zahn (1997), Maeder (1997). The effects of rotation on the mass loss rates is taken into account as explained in Maeder & Meynet (2000).

Let us stress also that these models are able to account for many observational constraints that non-rotating models cannot account for: they can reproduce surface enrichments (Heger & Langer 2000; Meynet & Maeder 2000), the blue to red supergiant ratios at low metallicity (Maeder & Meynet 2001), the variation with the metallicity of the Wolf-Rayet populations and of the number ratios of type Ibc to type II supernovae (Meynet & Maeder 2005a).

In the right part of Fig. 1, the evolution of the surface velocity for a $20 M_{\odot}$ stellar model at solar metallicity with $v_{\text{ini}} = 300 \text{ km s}^{-1}$ is shown (see the continuous line). Interestingly we note that the evolution of the surface velocity given by consistently taking into account the above transport mechanisms is not very far from the solid body rotation case, except at the very beginning and at the end of the Main Sequence phase.

At the beginning, the differentially rotating model presents a decrease of the surface velocity, not shown by the solid body rotation model. This initial decrease is due to the action of the meridional currents, which build up a gradient of Ω inside the star, transporting angular momentum from the outer regions to the inner ones. This slows down the surface of the star. Then, in the interior shear turbulence becomes active and erodes the gradients built by the meridional circulation. Under the influence of these two counteracting effects the Ω -profile converges toward an equilibrium configuration. This occurs on a very small timescale (a few percents of the Main-Sequence lifetime, see Denis-senkov et al. 1999). After this short phase, the variation of Ω in the radiative zone continues to be shaped by shear turbulence, meridional circulation and the change of stellar structure (expansion/contraction of the stellar layers).

At the end of the Main Sequence phase, when the star is older than about 9 Myr, the surface velocity rapidly decreases. This is a consequence of the mass loss rate recipe we used in this computation (Vink et al. 2000; 2001) which shows important enhancement of the mass loss rates when some critical effective temperature are crossed (bistability limits, see the above references). In absence of such strong stellar winds, the surface velocity would increase during this phase.

From this computation we can deduce the following results: first, during the Main-Sequence phase the transport mechanisms are efficient enough to maintain a relatively weak gradient of Ω inside the star (see the left part of Fig. 3). The situation is thus not too far from the solid body rotation case. Let us however note that the gradients of Ω , although modest, are sufficient enough to drive chemical mixing. These models predict changes of the surface abundances during the Main-Sequence phase well in agreement with what is observed (Heger and Langer 2000; Meynet & Maeder 2000; Maeder and Meynet 2001). Second, this numerical example illustrates the importance of the mass loss in shaping the evolution of the surface velocity (see also the discussion below and Fig. 2). Third, such models, starting with a higher initial velocity (typically above $\sim 350 \text{ km s}^{-1}$) would easily reach the critical limit during the Main-Sequence phase (see the results shown in Meynet and Maeder 2005b).

What does happen after the Main-Sequence phase ? The evolution speeds up and the variation of Ω inside the star is mainly governed by the local conservation of the angular momentum. We just saw in Sect. 3 above that, in situation where the radius grows up, this makes the surface velocity to evolve

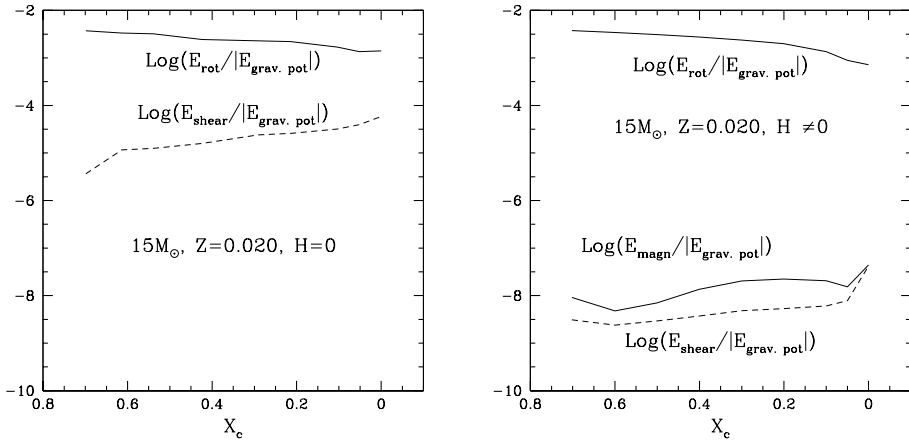


Figure 5. *Left* : Evolution of rotating kinetic energy, of excess energy in the shear for a $15 M_{\odot}$ stellar model at solar metallicity, with $v_{\text{ini}} = 300 \text{ km s}^{-1}$ without magnetic field. The energies are given as fraction of the gravitational energy. *Right* : The same as the left part but for model with rotation and magnetic field. The energy in the magnetic field is also indicated.

away from the critical limit. Only when the star contracts, for instance when a blue loop occurs in the HR diagram, may the star reach the critical limit (Heger & Langer 1998). This would be a possible scenario for the occurrence of B[e] stars, however as discussed by Langer & Heger (1998), this scenario would predict a short B[e] phase (only some 10^4 years) with correspondingly small amounts of mass lost.

Since such stars would have had their surface abundances changed by the deep outer convective zone appearing at the red supergiant phase, one expects that their surface abundance be highly enriched in CNO-processed material: as a numerical example, the N/C and N/O ratios at the surface of a $9 M_{\odot}$ stellar model at solar metallicity, with an initial rotation of $v_{\text{ini}} = 300 \text{ km s}^{-1}$ are enhanced by factors equal to 2.5 and 2.0 respectively during the first crossing of the HR gap from the blue to the red. These two ratios become 8.5 and 5.3 on the blue loop after a red supergiant stage. The models without rotation would predict for these ratios the following values: first crossing, no enhancement for both ratios; on the blue loop, enhancement factors of 5 and 3.5 respectively (Meynet & Maeder 2003). This numerical example shows that whatever the initial rotation velocity, models would predict some CNO-processed material at the surface if the star comes back from a red supergiant stage, secondly, rotation reinforces the surface enrichment on the blue loop with respect to non-rotating models.

Let us now see what happens to more massive stars. In Fig. 2, the evolution of the surface velocity for various $60 M_{\odot}$ stellar models at two different metallicities is shown. We see that at solar metallicity, the mass loss rates are so high that, even starting with an initial velocity of 500 km s^{-1} , the star does not reach the critical limit. The situation is quite different at low Z , due to the metallicity dependence of the mass loss rates (here we used $\dot{M}(Z) = (Z/Z_{\odot})^{\alpha} \dot{M}(Z_{\odot})$ with α equal to 0.5 as devised by Kudritzki & Puls 2000). Indeed, at low Z

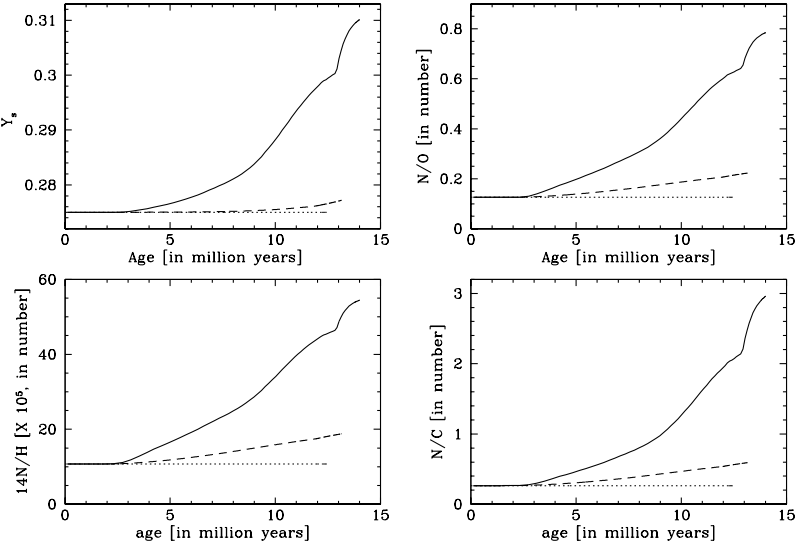


Figure 6. Time evolution of the surface helium content Y_s in mass fraction, of the N/O, N/H and N/C in mass fraction for various models: The dotted line applies to model without rotation, the short-broken line to model with rotation ($v_{\text{ini}} = 300 \text{ km s}^{-1}$) but without magnetic fields, the continuous line to model with rotation ($v_{\text{ini}} = 300 \text{ km s}^{-1}$) and magnetic fields.

little amounts of mass are removed by stellar winds, therefore little amounts of angular momentum. As a consequence, the angular momentum brought to the surface by the meridional circulation is not removed and accelerate the outer layers. Starting with $v_{\text{ini}} = 300 \text{ km s}^{-1}$, the star reaches the critical limit at the end of the Main-Sequence phase. Starting with an initial velocity of 800 km s^{-1} , the reaching of the critical limit occurs at a much earlier time.

For still higher initial masses, the stellar luminosity approaches the Eddington limit and, as explained above, the critical velocity becomes smaller than the value given by Eq. (1). The star may reach the $\Omega\Gamma$ -limit and lose very high amounts of mass (Maeder & Meynet 2000). Interestingly, in the HR diagram, the observed position of the de Jager or Humphreys-Davidson limit coincides with the position where this $\Omega\Gamma$ -limit would occur. This may be an indication that in the physics underlying this limit, both rotation and supra-Eddington luminosity play an important role.

5. Evolution of the surface velocity in models with shellular rotation and magnetic field

Spruit (2002) has proposed a dynamo mechanism operating in stellar radiative layers in differential rotation. This dynamo is based on the Tayler instability, which is the first one to occur in a radiative zone (Tayler 1973; Pitts & Tayler 1986). Even a very weak horizontal magnetic field is subject to Tayler instability, which then creates a vertical field component, which is wound up by differential rotation. As a result, the field lines become progressively closer

and denser and thus a strong horizontal field is created at the energy expense of differential rotation.

In a first paper (Maeder & Meynet 2003), we have shown that in a rotating star a magnetic field can be created during MS evolution by the Spruit dynamo. We have examined the timescale for the field creation, its amplitude and the related diffusion coefficients. The clear result is that magnetic field and its effects are quite important. In the second paper (Maeder & Meynet 2004), a generalisation of the equations of the dynamo has been developed. The solutions fully agree with Spruit's solution in the two limiting cases this author has considered (Spruit 2002), i.e. "Case 0" when the μ -gradient dominates and "Case 1" when the T -gradient dominates with large non-adiabatic effects. Our more general solution encompasses all cases of μ - and T -gradients, as well as all cases from the fully adiabatic to non-adiabatic solutions. In a last paper (Maeder & Meynet 2005), we examine the effects of the magnetic field created by Tayler-Spruit dynamo in differentially rotating stars. Magnetic fields of the order of a few 10^4 G are present through most the stellar envelope, with the exception of the outer layers. The diffusion coefficient for the transport of angular momentum is very large and it imposes nearly solid body rotation during the MS phase. This can be seen in Fig. 3 where are compared the evolutions of the angular velocity inside models with and without magnetic fields.

The surface velocities resulting from these two models are shown in Fig. 4. Except at the end of the Main Sequence phase, the model with magnetic field is strictly equivalent to the solid body rotation case.

Does the model with magnetic field predict surface enrichments ? Shear turbulence in magnetic models is very weak due to the flatness of the Ω internal profile. The excess of the energy in the shear in the magnetic model is only a few ten thousandths of the excess of the energy in the shear in the non-magnetic one (see Fig. 5). On the other hand, solid body rotation drives meridional circulation currents which are much faster than usual and leads to much larger diffusion coefficients than the shear diffusivity and than the magnetic diffusivity for the chemical species. As a consequence, the surface enrichments obtained in the models with rotation and magnetic fields are higher than in models with rotation only (see Fig. 6).

6. Conclusion

Be stars might be the natural outcome of stars with initial rotational velocity in the upper tail of the initial velocity distribution. Depending on when the critical limit is reached, one expects more or less high surface enrichments. If the critical limit is reached very early during the Main-Sequence phase, no enrichment is expected, while if the critical limit is reached at the end of the Main-Sequence phase, high N/C and N/O ratios are expected. At solar metallicity, for initial masses superior to about $50 M_\odot$, mass loss rates prevent the stars to reach the critical limit. The lower initial value for reaching the critical limit is likely limited by variation of the distribution of the initial velocities.

After the Main-Sequence phase, the variation of Ω inside the star is governed by the local conservation of the angular momentum. In phases during which the radius expands, this makes the surface velocity to evolve away from the

critical limit. In contracting phases, the reverse occurs. In the frame of single star evolution models, B[e] could be in a stage on a blue loop where the star contracted from a previous red supergiant phase. In that case, the surface is predicted to be enriched in CNO processed material.

The effects of magnetic fields in this context remain to be studied. However, already at this stage, it appears that magnetic field will facilitate the reaching of the critical limit.

References

Denissenkov, P.A., Ivanova, N.P., Weiss, A. 1991, A&A, 341, 181
 Glatzel, W. 1998, A&A, 339, L5
 Heger, A., Langer, N. 1998a, A&A, 334, 210
 Heger, A., Langer, N. 2000, ApJ, 544, 1016
 Hirschi, R., Maeder, A., Meynet, G. 2003, in *Stellar Rotation*, IAU Symp. 215, A. Maeder & P. Eeenens (eds.), ASPC, p. 510
 Kippenhahn, R., Thomas, H.C. 1970, in *Stellar Rotation*, IAU Coll. 4, Ed. A. Slettebak, p. 20
 Kudritzki R.P., Puls J. 2000, ARAA, 38, 613
 Langer, N. 1998, A&A, 329, 551
 Langer, N., Heger, A. 1998, in B[e] stars, A.M. Hubert & C. Jaschek (eds.), Ap&SS, 233, 235
 Maeder A. 1997, A&A, 321, 134
 Maeder, A. 1999, A&A, 347, 185
 Maeder, A., Meynet, G. 2000, A&A, 361, 159
 Maeder, A., Meynet, G. 2001, A&A, 373, 555
 Maeder, A., Meynet, G. 2003, A&A, 411, 543
 Maeder, A., Meynet, G. 2004, A&A, 422, 225
 Maeder, A., Meynet, G. 2005, A&A, 440, 1041
 Maeder A., Zahn J.P. 1998, A&A, 334, 1000
 Meynet, G., Maeder, A. 1997, A&A, 321, 465
 Meynet, G., Maeder, A. 2000, A&A, 361, 101
 Meynet, G., Maeder, A. 2003, A&A, 404, 975
 Meynet, G., Maeder, A. 2005a, A&A, 429, 581
 Meynet, G., Maeder, A. 2005b, in *The Nature and Evolution of Disks Around Hot Stars*, R. Ignace and K. G. Gayley (eds.), ASP Conf Ser. 337, p.15
 Pelupessy, I., Lamers, H.J.G.L.M., Vink, J.S. 2000, ApJ, 359, 695
 Pitts, E., Tayler, R.J. 1986, MNRAS, 216, 139
 Sackmann, I.-J., Anand, S.P.S. 1970, ApJ, 162, 105
 Spruit, H.C. 2002, A&A, 381, 923
 Talon, S., Zahn, J.P. 1997 , A&A, 317, 749
 Tayler, R.J. 1973, MNRAS, 161, 365
 Vink, J.S., de Koter, A., Lamers, H.J.G.L.M. 2000, A&A, 362, 295
 Vink, J.S., de Koter, A., Lamers, H.J.G.L.M. 2001, A&A, 369, 574
 von Zeipel, H. 1924, MNRAS, 84, 665
 Zahn, J.P. 1992, A&A, 265, 115
 Zickgraf, F.-J. 2000, in IAU Coll. 175, Myron A. Smith and Huib F. Henrichs (eds), ASPC, 214, p. 26